CATASTROPHIC DISRUPTION AND MOMENTUM TRANSFER IN HIGH-SPEED IMPACTS,

D.R. Davis and S.J. Weidenschilling, Planetary Sci. Inst.,Tucson, AZ.

Successful modeling of the collisional evolution of asteroids and planetesimals requires knowledge of collisional outcomes. Recently, we have been carrying out an experimental impact program designed to gather data on results of catastrophic disruption and momentum transfer by high speed collisions. This experimental program is an integral part of our studies of the formation and evolution of the solar system. Specifically, we aim to measure fragment size, velocity, and rotational distributions resulting from catastrophic destruction of concrete spheres and rock targets, and to measure the horizontal momentum imparted to a surface by cratering impacts at oblique angles.

A. Catastrophic Impact Experiments. These experiments address outcomes of catastrophic collisions -- sizes, velocities, and rotation rates of the fragments. A series of experiments (Table 1) was carried out in 1981 at the Ames Vertical Gun Facility (AVGF) and in 1980 at the Santa Ana Impact Facility (SAIF) using concrete spheres having different compressive strengths. Concrete was chosen since it is a reasonably good analog for rocky materials and can be produced to have any selected strength over a wide range. As seen in Table 1, we used targets with strength ranging over a factor of >20.

The size of the largest fragment, expressed as a fraction of the initial target mass, was compared with data obtained by Hartmann (1978) for silicate targets. The earlier data were obtained at impact speeds of a few 10's of meters/sec, whereas the current data is for speeds from several hundreds of meters/sec to 2¼ km/sec. We find that the concrete spheres are similar to basalts and igneous rock targets in terms of fragmentation properties: the new results generally agree with the earlier data in the variation of the largest fragment size as a function of collisional energy. They suggest that an "impact strength" (defined as the kinetic energy per cm^3 of target material required to remove 50% of the initial mass) of 5×10^6 $ergs/cm^3$ is appropriate for targets of crushing strength 3.5×10^8 $dynes/cm^2$.

Our collisional models (Greenberg et al., 1978) have assumed that the available energy is partitioned equally between the two bodies involved in a collision. This was verified experimentally by Hartmann for the case when the strength of the target and projectile are comparable. However, the assumption may not hold when there is a large strength difference between the two bodies. Our results suggest that for the same specific energy, a projectile significantly stronger than the target (steel projectile, concrete target) is more effective at comminuting the target than relatively weaker projectiles (Al or glass). Shots AV-616 and AV-617, e.g., used Al projectiles and had comparable specific energy and yielded largest fragments that contained 80% and 69% of the initial target mass. Shot AV-615, with the same specific energy but a steel projectile, produced a largest fragment of only 29% of the initial target mass. Impact experiments with concrete spheres were filmed by two Nova cameras at 4500 frames/sec to measure the ejecta velocity and rotational distribution. Analysis of these films by mapping the motion of individual fragments from frame to frame in both camera views is underway using a digital image analysis system.

B. Comparison with Computational Algorithms. One goal of our experimental program is to provide data for improving the collisional outcome computations in our numerical planet-building model (Greenberg et al., 1978). Comparisons were made between experimental results and theoretical models for cases of cratering, barely catastrophic collisions, and super-catastrophic collisions. Table 1 compares the computed and actual fractional mass of the largest fragment, M_ℓ/M_o, calculated using the algorithm of Greenberg et al. For cratering and barely catastrophic impacts, the predicted mass is in good agreement with the experimental outcome. While there is a greater variance between predicted and actual largest fragment masses for super-catastrophic collisions, the differences are within the expected variation of experimental outcomes. In all cases, the outcome predicted by the algorithm of Greenberg *et al.* -- cratering, barely castrophic or super-catastrophic -- was verified by the experimental results.

C. Momentum Transfer By Oblique Impacts. A series of oblique impact experiments at the AVGF was performed in June, 1981. The target consisted of a wooden box filled with sand, suspended by cables as a ballistic pendulum. Shots were fired into the sand at various zenith angles, and the resulting oscillations of the pendulum recorded on film. Amplitudes were measured by a scale attached to the box and a fixed pointer. The horizontal component of momentum was calculated by Fourier analysis of the oscillation amplitudes.

Seventeen shots produced usable results, covering zenith angles from 30° to 75° in 15° increments. Projectiles were spheres of Pyrex, Al, and steel. Impact velocities ranged from 1.1 to 2.3 km s^{-1}. Results are plotted in Fig. 1. The efficiency of momentum transfer, ζ, is defined as the fraction of the projectile's horizontal component of momentum transmitted to the target. We find ζ decreases monotonically with zenith angle θ, but is not well-fitted by a power of cos θ; rather, it appears linear in θ. There is no significant correlation with projectile velocity or material properties. Apparently impact angle is the dominant factor.

REFERENCES: Greenberg, R., Wacker, J., Hartmann, W.K., and Chapman, C.R. (1978), *Icarus* 35, 1-26. Hartmann, W.K. (1978), *Icarus* 33, 50-61.

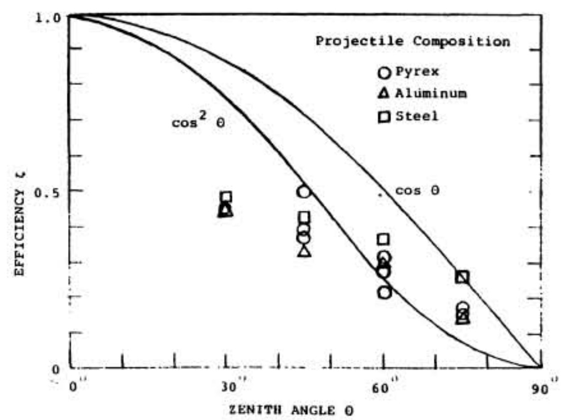

Fig. 1: Efficiency of momentum transport vs. zenith angle

TABLE 1: RESULTS OF CATASTROPHIC COLLISION EXPERIMENTS

EXPERIMENT Number	TARGET MASS (kg)	DESIGN STR. (dyne/cm^2)	MEASURED STR. (dyne/cm^2)	PROJECTILE Mass (g)	IMPACT SPEED (m/s)	ENERGY (erg)	M_ℓ/M_o (calc)	M_ℓ/M_o (actual)
SA-1	1.482	3.5(8)	3.2(8)	1.119	~787	3.5(9)	1.0	0.93
SA-2	1.478	3.5(8)	3.2(8)	1.078	787	3.3(9)	1.0	0.96
SA-3	1.493	3.5(8)	3.2(8)	1.118	1296	9.4(9)	0.47	0.90
SA-4	1.304	3.5(8)	3.2(8)	5.107	851	1.8(10)	0.18	0.09
SA-5	1.445	3.5(8)	3.2(8)	5.298	581	8.9(9)	0.48	0.55
SA-6	1.327	3.5(8)	3.2(8)	5.111	793	1.6(10)	0.21	0.07
SA-7	1.344	3.5(8)	4.2(8)	4.830	476	5.5(9)	0.80	0.92
SA-8	1.449	3.5(8)	4.2(8)	5.090	627	1.0(10)	0.41	0.58
SA-9	1.386	3.5(8)	3.4(8)	5.390	1042	2.9(10)	0.11	0.22
SA-10	1.332	3.5(8)	3.4(8)	14.100	1018	7.3(10)	0.03	0.03
SA-11	1.554	7.0(8)	6.0(8)	5.320	851	1.9(10)	0.02	0.11
SA-12	1.032	3.5(7)	2.8(7)	1.193	614	2.2(9)	1.0	N/A
SA-13	1.060	3.5(7)	2.8(7)	5.440	1035	2.9(10)	0.08	0.01
AV-614	1.329	5.0(8)		1.043	1520	1.2(10)	0.30	0.09
AV-615	1.354	5.0(8)		1.043	1308	8.9(9)	0.45	0.29
AV-616	1.347	5.0(8)		0.375	2130	8.5(9)	0.47	0.80
AV-617	1.329	5.0(8)		0.375	2240	9.4(9)	0.41	0.69
AV-618	1.315	5.0(8)		1.044	1420	1.1(10)	0.35	0.13
AV-619	0.932	5.0(8)		1.043	1990	2.1(10)	0.10	0.02
AV-626	0.912	5.0(8)		66.741	N/A	N/A	----	0.45